Chaotic synchronization of irregular complex network with hysteretic circuit-like oscillators in hamiltonian form and its application in private communications

E. Garza-González, C. Posadas-Castillo, and A. Rodríguez-Liñan
Universidad Autónoma de Nuevo León,
Av. Pedro de Alba s/n, Cd. Universitaria, C.P. 66451, San Nicolás de los Garza N.L., México.
e-mail: egarza.ikaro@gmail.com; cornelio.posadascs@uanl.edu.mx; angel.rodriguezln@uanl.edu.mx

C. Cruz-Hernández
Scientific Research and Advanced Studies Center of Ensenada.
e-mail: ccruz@cicese.mx

Received 25 August 2015; accepted 30 October 2015

In this paper, a study on chaotic synchronization of an irregular network is made. Synchronization is achieved by using a modified Hamiltonian approach in a bidirectional irregular arrayed network made of 20 chaotic oscillators. The chaotic oscillator used as example is the Hysteretic circuit. Afterwards the concept is used in chaotic encryption to send secured confidential analog information. As a result, an image is encrypted using additive chaotic encrytion with two channels.

Keywords: Chaotic synchronization; hysteretic circuit; generalized hamiltonian system; private communication; complex networks.

En este trabajo, un estudio de la sincronización caótica de una red irregular es realizada. La sincronización es alcanzada al usar una modificación al enfoque Hamiltoniano sobre una red bidireccional irregular creada por 20 osciladores caóticos. El oscilador caótico usado como ejemplo es el circuito de Histeresis. Después, este concepto es usado en encriptamiento caótico para enviar información análoga confidencial de manera segura. Como resultado, una imagen es encriptada usando encriptamiento caótico aditivo de dos canales.

Descriptores: Sincronización caótica; circuito de histéresis; sistema hamiltoniano generalizado; comunicaciones privadas; redes complejas.

PACS: 05.45.-a; 05.45.Gg; 05.45.Pq; 05.45.Vx; 05.45.Xt

1. Introduction

In recent years, chaotic synchronization has received a special attention from the scientific community, due to the large number of applications and benefits that offers this phenomenon in human affairs. Many master-slave chaotic synchronization have been reported in the scientific literature, see *e.g.* [1-4] and references therein. However many systems in nature and in technology are composed by a large number of highly interconnected dynamical units, where their collective behaviors are completely different to the individual behavior of each dynamical units. Such systems generate very complicated dynamics, the so-called complex network systems, see *e.g.* [5,6]. In fact this behavior has been found in scientific article network [7,8], social relationships [9,10], ecology [11], metabolic networks [12], neural networks [13], among others. Due to this intrinsical properties, it has been used in secure communication systems as well, as seen in Refs. 14 to 17. However, the security level had to be increased due to recent investigations in decryption, which had made lots of these cryptosystems obsolete, [18,19].

To increase the security level, many of the cryptosystems turn into more complex systems or use a combination of techniques. Other approach can be by choosing a chaotic oscillator with a higher number of positive Lyapunov exponents, also called hyperchaotic [20-22], multi-scroll attractors [23,24], fractional order chaotic oscillators [25-27], or even systems in a generalized Hamiltonian form [28,29]. The Hamiltonian approach have been extended to networks in Ref. 30, by modelling the couplings as a complex network and having a coupling force as a scalar. Instead, we aim for a full Hamiltonian estimate-like model in which the gain of the network is described as a vector. This way each state has its own individual gain over the network.

The main goals of this paper are: *i*) to synchronize Hysteretic chaotic oscillators in their generalized Hamiltonian form. This chaotic oscillators are coupled in an irregular arrayed network using bidirectional connections (undirected graph). This objective is achieved using a modified Hamiltonian approach based on [31] and [32]. And, *ii*) to transmit an encrypted image message based on chaos synchronization using additive encryption.

The paper is organized as follows: Section 2 shows a brief summary on synchronization of complex networks. Section 3, describes synchronization via the Generalized Hamiltonian form and observer design. In Sec. 4 describes synchronization in complex networks using the Generalized Hamiltonian approach. By using computer simulations, the approach used is explained by means of the Hysteretic chaotic circuit in Sec. 5. In Sec. 6, a brief introduction on additive encryption with two channels is given; plus specifics on the image reconstruction algorithm. In Sec. 7 the results on the chaotic encryption scheme are shown. Finally, some conclusions are given in Sec. 8.

2. Synchronization of complex networks

2.1. Synchronization analysis

Synchronization is a process where many systems adjust a given property of their motion to a common behavior, due to coupling or forcing [33]. Consider a set of identical systems, defined by

$$\dot{\mathbf{x}}_i = f(x_i), \tag{1}$$

where $\dot{\mathbf{x}}_i = [x_{i1}, x_{i2}, ..., x_{in}]^\intercal \in \Re^n$, is the state variables of the oscillator i, f is a vector field defined in $\Re^n$ and $i = 1, 2, ..., N$ defines the different systems. The systems synchronize if

$$\lim_{t\to\infty} ||\mathbf{x}_i(t) - \mathbf{x}_j(t)|| = 0, \qquad \forall t \geq \tau, \tag{2}$$

where $i, j = 1, 2, ..., N$ represents all chaotic oscillators and $i \neq j$, $\mathbf{x}_i(t)$ and $\mathbf{x}_j(t)$ represents the states of the pair of chaotic oscillators i and j, where initial conditions $\mathbf{x}_i(0) \neq \mathbf{x}_j(0)$, and τ is the synchronization time. It is also said that the error vector of synchronization is defined with the expression:

$$e(t) = \mathbf{x}_i(t) - \mathbf{x}_j(t), \qquad \mathbf{x}_i, \mathbf{x}_j \in \Re^n, \tag{3}$$

synchrony exists if $e(t) = 0$. Although, it is possible that the error vector is not zero, but stays uniformly below a positive value of $\rho \in \Re$, as expressed by:

$$\lim_{t\to\infty} ||\mathbf{x}_i(t) - \mathbf{x}_j(t)|| \leq \rho. \tag{4}$$

For this paper, a set of identical systems are used coupled in a network. As such, it is possible to obtain all possible errors between any given oscillators in the network using (3), and by further inspection, observe if the network is fully synchronized. A better way to look at complete synchronization of the entire network is to use the root mean squared error e_{RMS}. This error provide a characteristic value for a quantity that is continuously changing. The aim in this paper is to synchronize all states of the oscillators in the network. Adjusting to it, the root mean squared error e_{RMS} is defined by [34]

$$e_{\text{RMS}} = \frac{1}{\sum_{l-1}^{N-1}(N-l)} \sqrt{\sum_{i=1}^{N-1} \sum_{j=i+1}^{N} \sum_{h=1}^{n} (x_{i,h} - x_{j,h})^2}, \tag{5}$$

where N is the amount of oscillators in the network, $h = 1, 2, ..., n$ represents the n states of the oscillators, $l, i = 1, 2, ..., N-1$, and $j = 2, 3, ..., N$ represent all oscillators in the network where $i \neq j$. The network is fully synchronized in all states if

$$e_{RMS} = 0, \tag{6}$$

therefore Eq. (2) holds.

2.2. Complex dynamical network

Consider a dynamical network [32], that is made of N identical linearly and diffusively coupled n-dimensional oscillators as (1). The state equations of the network is defined as

$$\dot{x}_i = f(x_i) + c \sum_{j=1}^{N} a_{ij} \mathbf{\Gamma} x_j, \quad i = 1, 2, ..., N, \tag{7}$$

where the constant $c > 0$ is the coupling strenght of the network. $\mathbf{\Gamma} \in \Re^{n\times n}$ is a constant matrix and it is assumed that $\mathbf{\Gamma} = diag(r_1, r_2, ..., r_n)$ is a diagonal matrix with $r_i = 1$ for a particular i and $r_j = 0$ for $j \neq i$. This means that the coupled oscillators are linked through their i-th state variables. The coupling matrix $\mathbf{A} = (a_{ij}) \in \Re^{N\times N}$ represents the coupling configuration of the network. If there is a connection between oscillator i and oscillator j, then $a_{ij} = 1$; otherwise, $a_{ij} = 0$ $(i \neq j)$. The diagonal elements of $\mathbf{A}$ are defined as:

$$a_{ij} = -\sum_{j=1, j\neq i}^{N} a_{ij} = -\sum_{j=1, j\neq i}^{N} a_{ji}, \quad i = 1, 2, ..., N. \tag{8}$$

If the degree of oscillator i is k_i, then

$$a_{ii} = -k_i, \qquad i = 1, 2, ..., N. \tag{9}$$

The complex dynamical network in (7), can achieve synchronization, if

$$x_1(t) = x_2(t) = \ldots = x_N(t), \qquad \text{as} \qquad t \to \infty, \tag{10}$$

this as portrait in the definition of synchronization in (2).

3. Hamiltonian systems

The dynamical systems problem can be approach using an energy based model, such as the Hamiltonian systems theory. In previews works, it has been shown chaotic oscillators configured in a master-slave arrangement, can achieve synchronization using a Hamiltonian method [31]. Consider one dynamical system like (1), it can be rewritten as its Generalized Hamiltonian canonical form as [31]

$$\begin{aligned} \dot{x} &= \mathbf{J}(y)\frac{\partial H}{\partial x} + (\mathbf{I} + \mathbf{S})\frac{\partial H}{\partial x} + \mathbf{F}(y), \\ y &= \mathbf{C}\frac{\partial H}{\partial x}, \end{aligned} \tag{11}$$

where $\mathbf{J}(y)\partial H/\partial x$ exhibits the conservative part of the system. $\mathbf{S}$ is a constant symmetric matrix, not necessarily of definite sign. $\mathbf{I}$ is a constant skew symmetric matrix. $\mathbf{F}(y)$ represents a locally destabilizing vector field. The vector variable y is referred to as the system output. The matrix $\mathbf{C}$ is a constant matrix. $H(x)$ denotes a smooth energy function which is globally positive $\Re^n$. The columns gradient vector of H, denoted by $\partial H/\partial x$, is assumed to exist everywhere.

It is denoted that the estimate of the state vector x by ξ, and the Hamiltonian energy function $H(\xi)$ to the particularization of H in terms of ξ. η is denoted as the estimated output, computed in terms of the estimated state ξ. The dynamic nonlinear state observer for the system (11) will be as follows:

$$\dot{\xi} = \mathbf{J}(y)\frac{\partial H}{\partial \xi} + (\mathbf{I}+\mathbf{S})\frac{\partial H}{\partial \xi} + \mathbf{F}(y) + \mathbf{K}(y-\eta),$$
$$\eta = \mathbf{C}\frac{\partial H}{\partial \xi}, \tag{12}$$

where **K** is a constant vector, known as the observer gain. For the following theorems $\mathbf{I}+\mathbf{S}=\mathbf{W}$, when needed.

Theorem 3.1 [31] *The state x of the nonlinear system* (11) *can be globally, exponentially, asymptotically estimated by the state ξ of an observer of the form* (12)*, if the pair of matrices $(\mathbf{C},\mathbf{W})$, or the pair $(\mathbf{C},\mathbf{S})$, is either observable or, at least, detectable. An observability condition on either of the pairs $(\mathbf{C},\mathbf{W})$, or $(\mathbf{C},\mathbf{S})$, is a sufficient but not necessary condition for asymptotic state reconstruction.*

Theorem 3.2 [31] *The state x of the nonlinear system* (11) *can be globally, exponentially, asymptotically estimated by the state ξ of an observer of the form* (12)*, if and only if there exist a constant matrix K such that the symmetric matrix*

$$[\mathbf{W}-\mathbf{KC}] + [\mathbf{W}-\mathbf{KC}]^\intercal = [\mathbf{S}-\mathbf{KC}] + [\mathbf{S}-\mathbf{KC}]^\intercal$$
$$= 2\left[\mathbf{S} - \frac{1}{2}(\mathbf{KC} + \mathbf{C}^\intercal\mathbf{K}^\intercal)\right], \tag{13}$$

is negative definite.

4. Hamiltonian networks

One of the objectives of this paper, is to extend said approach in Sec. 3 to a network of multiple oscillators. Based on the model (7) in Ref. 32 as a framework for the notation, a model of a Hamiltonian network has been obtained. The dynamics of a complex network where the oscillators are given in Hamiltonian form are determined as follows:

$$\dot{x}_i = \mathbf{J}(y_i)\frac{\partial H}{\partial x_i} + (\mathbf{I}+\mathbf{S})\frac{\partial H}{\partial x_i} + \mathbf{F}(y_i) + \mathbf{K}\sum_{j=1}^{N} a_{ij}y_j,$$
$$y_i = +\mathbf{C}\frac{\partial H}{\partial x_i}, \tag{14}$$

where $i = 1, 2, ..., N$ represents all the chaotic oscillators, $\dot{x}_i = (x_{i1}, x_{i2}, ..., x_{in})^\intercal \in \Re^n$ is the state vector of the i-th oscillator, $\mathbf{K} = [K_1 \quad K_2 \quad K_3]^\intercal$ is a constant vector $\in R^n$ and is the gain of the network, $\mathbf{A} = (a_ij) \in \Re^{N\times N}$ is called coupling matrix and represents the coupling configuration of the network, $\partial H/\partial x_i$ is the columns gradient vector $\in \Re^n$ and is assumed to exist everywhere. For the network case, the following notation will be used:

$$\frac{\partial H}{\partial x_i} = \left[\frac{\partial H}{\partial x_{i,1}} \; \frac{\partial H}{\partial x_{i,2}} \cdots \frac{\partial H}{\partial x_{i,n}}\right]^\intercal. \tag{15}$$

To easily note the difference between the oscillator number i and the states, a comma will be placed.

5. Hysteretic chaotic circuit in an irregular network

Consider the following nonlinear equations for a hysteretic chaotic circuit described by

$$\begin{cases} \dot{x}_1 = x_2 + \gamma x_1 + g x_3, \\ \dot{x}_2 = -\omega x_1 - \delta x_2, \\ \varepsilon \dot{x}_3 = (1 - x_3^2)(s x_1 + x_3) - \beta x_3. \end{cases}$$

A chaotic dynamic is achieved, if the parameters used are: $\gamma = 0.2$, $g = 2$, $\omega = 10$, $\delta = 0.001$, $s = 1.667$, $\beta = 0.001$, $\varepsilon = 0.3$ [31]. The chaotic attractor is shown in Fig. 1.

The generalized Hamiltonian form of the Hysteretic chaotic circuit (16) is expressed as [31]:

$$\begin{bmatrix} \dot{x}_1 \\ \dot{x}_2 \\ \dot{x}_3 \end{bmatrix} = \begin{bmatrix} 0 & \frac{1}{2}(1+\omega) & \frac{1}{2\varepsilon}(g-s) \\ -\frac{1}{2}(1+\omega) & 0 & 0 \\ -\frac{1}{2\varepsilon}(g-s) & 0 & 0 \end{bmatrix} \frac{\partial H}{\partial x}$$
$$+ \begin{bmatrix} \gamma & \frac{1}{2}(1-\omega) & \frac{1}{2\varepsilon}(g+s) \\ \frac{1}{2}(1-\omega) & -\delta & 0 \\ \frac{1}{2\varepsilon}(g+s) & 0 & -\frac{1}{\varepsilon^2}(\beta-1) \end{bmatrix} \frac{\partial H}{\partial x}$$
$$+ \begin{bmatrix} 0 \\ 0 \\ -x_3^2(x_3 + s x_1) \end{bmatrix},$$
$$y = [1 \quad 0 \quad 0]\frac{\partial H}{\partial x}. \tag{16}$$

The **C** and **S** matrices are given by

$$\mathbf{C} = [1 \quad 0 \quad 0],$$
$$\mathbf{S} = \begin{bmatrix} \gamma & \frac{1}{2}(1-\omega) & \frac{1}{2\varepsilon}(g+s) \\ \frac{1}{2}(1-\omega) & -\delta & 0 \\ \frac{1}{2\varepsilon}(g+s) & 0 & -\frac{1}{\varepsilon^2}(\beta-1) \end{bmatrix}.$$

The pair (**C**,**S**) is observable, and hence detectable. Therefore Theorem 3.1 holds. The energy function of the Hysteretic chaotic circuit is defined by

$$H(x) = \frac{1}{2}(x_1^2 + x_2^2 + \varepsilon x_3^2). \tag{17}$$

Consider an irregular network of 20 Hysteretic chaotic oscillators in generalized Hamiltonian form as in Eq. (16), see Fig. 1. By using (16) and (17) with the connection topology like is shown in Fig. 2, the corresponding coupling matrix is given by

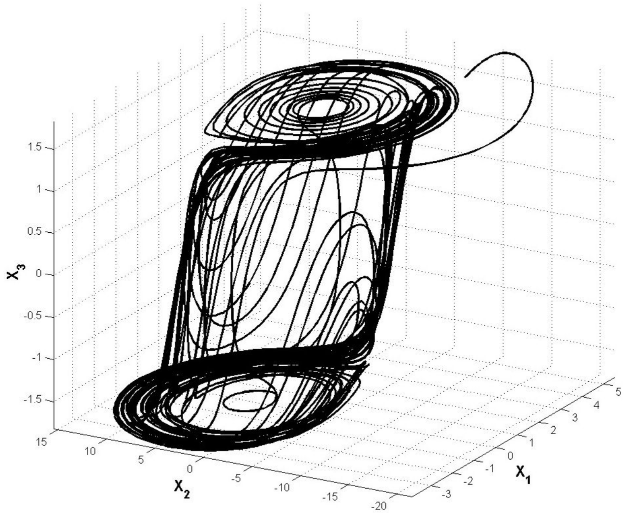

FIGURE 1. Chaotic attractor of the Hysteretic circuit chaotic oscillator projected onto the (x_1, x_2, x_3)-space.

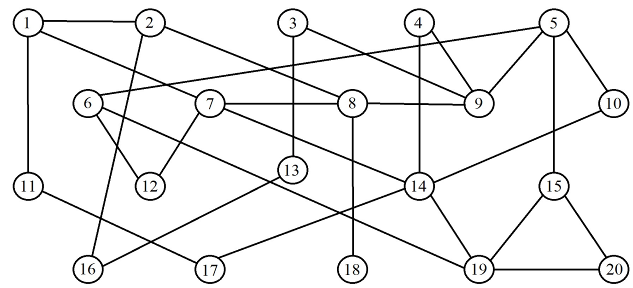

FIGURE 2. An irregular arrayed network connection topology consisting of 20 oscillators that will be used for the synchronization. The oscillators were arbitrary coupled.

$$\mathbf{A} = \begin{bmatrix}
-3 & 1 & 0 & 0 & 0 & 0 & 1 & 0 & 0 & 0 & 1 & 0 & 0 & 0 & 0 & 0 & 0 & 0 & 0 & 0 \\
1 & -3 & 0 & 0 & 0 & 0 & 0 & 1 & 0 & 0 & 0 & 0 & 0 & 0 & 0 & 1 & 0 & 0 & 0 & 0 \\
0 & 0 & -2 & 0 & 0 & 0 & 0 & 0 & 1 & 0 & 0 & 0 & 1 & 0 & 0 & 0 & 0 & 0 & 0 & 0 \\
0 & 0 & 0 & -2 & 0 & 0 & 0 & 0 & 1 & 0 & 0 & 0 & 0 & 1 & 0 & 0 & 0 & 0 & 0 & 0 \\
0 & 0 & 0 & 0 & -4 & 1 & 0 & 0 & 1 & 1 & 0 & 0 & 0 & 0 & 1 & 0 & 0 & 0 & 0 & 0 \\
0 & 0 & 0 & 0 & 1 & -3 & 0 & 0 & 0 & 0 & 0 & 1 & 0 & 0 & 0 & 0 & 0 & 0 & 0 & 0 \\
1 & 0 & 0 & 0 & 0 & 0 & -4 & 1 & 0 & 0 & 0 & 1 & 0 & 1 & 0 & 0 & 0 & 0 & 1 & 0 \\
0 & 1 & 0 & 0 & 0 & 0 & 1 & -4 & 1 & 0 & 0 & 0 & 0 & 0 & 0 & 0 & 0 & 1 & 0 & 0 \\
0 & 0 & 1 & 1 & 1 & 0 & 0 & 1 & -4 & 0 & 0 & 0 & 0 & 0 & 0 & 0 & 0 & 0 & 0 & 0 \\
0 & 0 & 0 & 0 & 1 & 0 & 0 & 0 & 0 & -2 & 0 & 0 & 0 & 1 & 0 & 0 & 0 & 0 & 0 & 0 \\
1 & 0 & 0 & 0 & 0 & 0 & 0 & 0 & 0 & 0 & -2 & 0 & 0 & 0 & 0 & 0 & 1 & 0 & 0 & 0 \\
0 & 0 & 0 & 0 & 0 & 1 & 1 & 0 & 0 & 0 & 0 & -3 & 1 & 0 & 0 & 0 & 0 & 0 & 0 & 0 \\
0 & 0 & 1 & 0 & 0 & 0 & 0 & 0 & 0 & 0 & 0 & 1 & -3 & 0 & 0 & 1 & 0 & 0 & 0 & 0 \\
0 & 0 & 0 & 1 & 0 & 0 & 1 & 0 & 0 & 1 & 0 & 0 & 0 & -5 & 0 & 0 & 1 & 0 & 1 & 0 \\
0 & 0 & 0 & 0 & 1 & 0 & 0 & 0 & 0 & 0 & 0 & 0 & 0 & 0 & -3 & 0 & 0 & 0 & 1 & 1 \\
0 & 1 & 0 & 0 & 0 & 0 & 0 & 0 & 0 & 0 & 0 & 0 & 1 & 0 & 0 & -2 & 0 & 0 & 0 & 0 \\
0 & 0 & 0 & 0 & 0 & 0 & 0 & 0 & 0 & 0 & 1 & 0 & 0 & 1 & 0 & 0 & -2 & 0 & 0 & 0 \\
0 & 0 & 0 & 0 & 0 & 0 & 0 & 1 & 0 & 0 & 0 & 0 & 0 & 0 & 0 & 0 & 0 & -1 & 0 & 0 \\
0 & 0 & 0 & 0 & 0 & 1 & 0 & 0 & 0 & 0 & 0 & 0 & 0 & 1 & 1 & 0 & 0 & 0 & -4 & 1 \\
0 & 0 & 0 & 0 & 0 & 0 & 0 & 0 & 0 & 0 & 0 & 0 & 0 & 0 & 1 & 0 & 0 & 0 & 1 & -2
\end{bmatrix}.$$

To construct the proposed arrangement shown in Fig. 2 (with 29 connections), we have used the coupling signals y_i, $i = 1, 2, ..., 20$ for the 20 oscillators. For this purpose, we have designed the input signals u_i, $i = 1, 2, ..., 20$ that explicitly are given by $u_1 = (-3y_{1,1} + y_{2,1} + y_{7,1} + y_{11,1})$, $u_2 = (y_{1,1} - 3y_{2,1} + y_{8,1} + y_{16,1})$, $u_3 = (-2y_{3,1} + y_{9,1} + y_{13,1})$, $u_4 = (-2y_{4,1} + y_{9,1} + y_{14,1})$, $u_5 = (-4y_{5,1} + y_{6,1} + y_{9,1} + y_{10,1} + y_{15,1})$, $u_6 = (y_{5,1} - 3y_{6,1} + y_{12,1} + y_{19,1})$, $u_7 = (y_{1,1} - 4y_{7,1} + y_{8,1} + y_{12,1} + y_{14,1})$, $u_8 = (y_{2,1} + y_{7,1} - 4y_{8,1} + y_{9,1} + y_{18,1})$, $u_9 = (y_{3,1} + y_{4,1} + y_{5,1} + y_{8,1} - 4y_{9,1})$, $u_{10} = (y_{5,1} - 2y_{10,1} + y_{14,1})$, $u_{11} = (y_{1,1} - 2y_{11,1} + y_{17,1})$, $u_{12} = (y_{6,1} + y_{7,1} - 3y_{12,1} + y_{13,1})$, $u_{13} = (y_{3,1} + y_{12,1} - 3y_{13,1} + y_{16,1})$, $u_{14} = (y_{4,1} + y_{7,1} + y_{10,1} - 5y_{14,1} + y_{17,1} + y_{19,1})$, $u_{15} = (y_{5,1} - 3y_{15,1} + y_{19,1} + y_{20,1})$, $u_{16} = (y_{2,1} + y_{13,1} - 2y_{16,1})$, $u_{17} = (y_{11,1} + y_{14,1} - 2y_{17,1})$, $u_{18} = (y_{8,1} - y_{18,1})$, $u_{19} = (y_{6,1} + y_{14,1} + y_{15,1} - 4y_{19,1} + y_{20,1})$, $u_{20} = (y_{15,1} + y_{19,1} - 2y_{20,1})$.

Using (14), the network is written as:

$$N_1 \left\{ \begin{aligned} \begin{bmatrix} \dot{x}_{1,1} \\ \dot{x}_{1,2} \\ \dot{x}_{1,3} \end{bmatrix} &= \begin{bmatrix} 0 & \frac{1}{2}(1+\omega) & \frac{1}{2\varepsilon}(g-s) \\ -\frac{1}{2}(1+\omega) & 0 & 0 \\ -\frac{1}{2\varepsilon}(g-s) & 0 & 0 \end{bmatrix} \frac{\partial H}{\partial x_1} \\ &+ \begin{bmatrix} \gamma & \frac{1}{2}(1-\omega) & \frac{1}{2\varepsilon}(g+s) \\ \frac{1}{2}(1-\omega) & -\delta & 0 \\ \frac{1}{2\varepsilon}(g+s) & 0 & -\frac{1}{\varepsilon^2}(\beta-1) \end{bmatrix} \frac{\partial H}{\partial x_1} + \begin{bmatrix} 0 \\ 0 \\ -x_{1,3}^2(x_{1,3}) + s x_{1,1} \end{bmatrix} + K u_1, \end{aligned} \right.$$

$$N_2 \begin{cases} \begin{bmatrix} \dot{x}_{2,1} \\ \dot{x}_{2,2} \\ \dot{x}_{2,3} \end{bmatrix} = \begin{bmatrix} 0 & \frac{1}{2}(1+\omega) & \frac{1}{2\varepsilon}(g-s) \\ -\frac{1}{2}(1+\omega) & 0 & 0 \\ -\frac{1}{2\varepsilon}(g-s) & 0 & 0 \end{bmatrix} \frac{\partial H}{\partial x_2} \\ \qquad + \begin{bmatrix} \gamma & \frac{1}{2}(1-\omega) & \frac{1}{2\varepsilon}(g+s) \\ \frac{1}{2}(1-\omega) & -\delta & 0 \\ \frac{1}{2\varepsilon}(g+s) & 0 & -\frac{1}{\varepsilon^2}(\beta-1) \end{bmatrix} \frac{\partial H}{\partial x_2} + \begin{bmatrix} 0 \\ 0 \\ -x_{2,3}^2(x_{2,3}) + s x_{2,1} \end{bmatrix} + K u_2, \end{cases}$$

$$\vdots$$

$$N_{20} \begin{cases} \begin{bmatrix} \dot{x}_{20,1} \\ \dot{x}_{20,2} \\ \dot{x}_{20,3} \end{bmatrix} = \begin{bmatrix} 0 & \frac{1}{2}(1+\omega) & \frac{1}{2\varepsilon}(g-s) \\ -\frac{1}{2}(1+\omega) & 0 & 0 \\ -\frac{1}{2\varepsilon}(g-s) & 0 & 0 \end{bmatrix} \frac{\partial H}{\partial x_{20}} \\ \qquad + \begin{bmatrix} \gamma & \frac{1}{2}(1-\omega) & \frac{1}{2\varepsilon}(g+s) \\ \frac{1}{2}(1-\omega) & -\delta & 0 \\ \frac{1}{2\varepsilon}(g+s) & 0 & -\frac{1}{\varepsilon^2}(\beta-1) \end{bmatrix} \frac{\partial H}{\partial x_{20}} + \begin{bmatrix} 0 \\ 0 \\ -x_{20,3}^2(x_{20,3}) + s x_{20,1} \end{bmatrix} + K u_{20}. \end{cases}$$

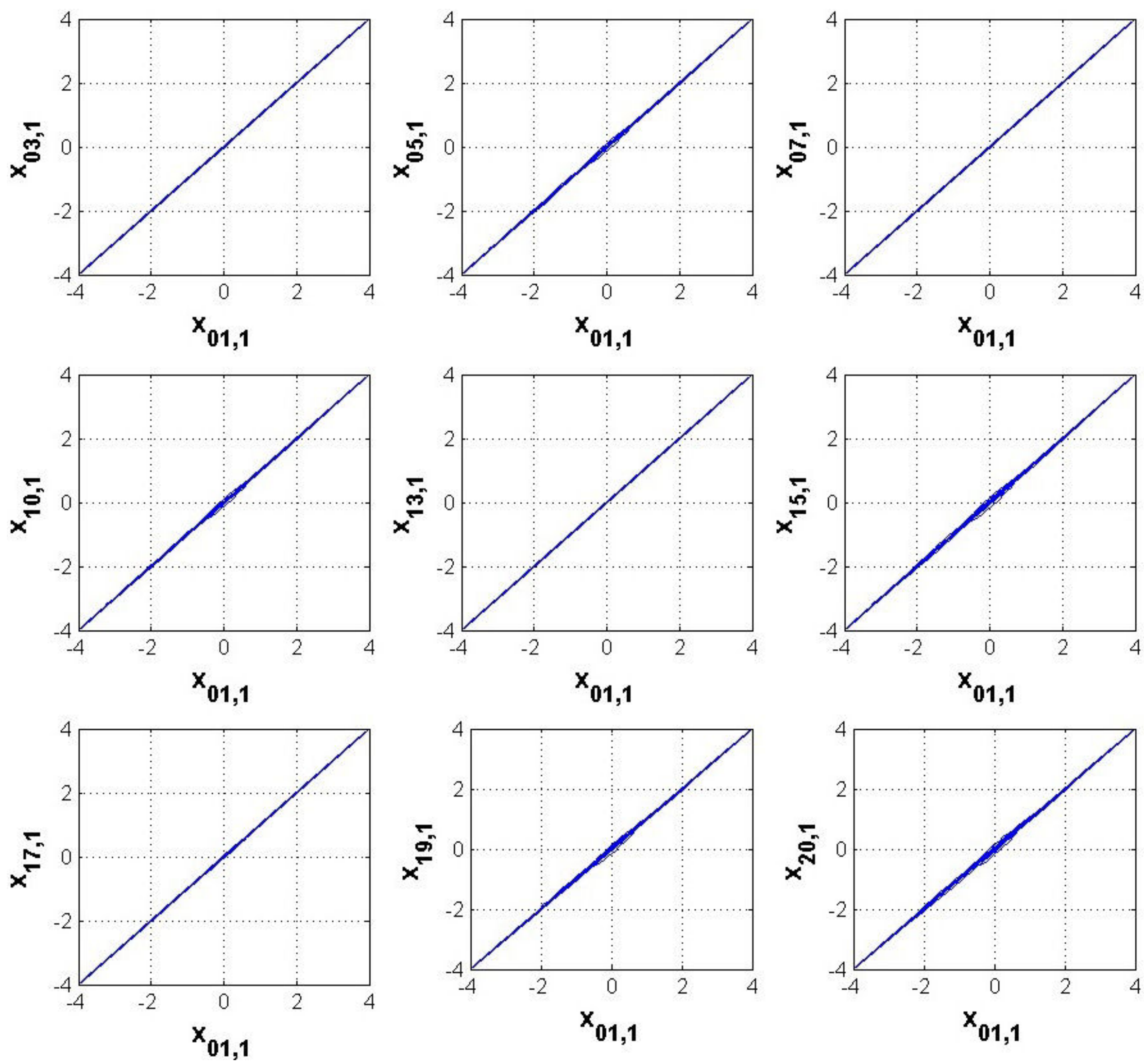

FIGURE 3. Phase plane of the state x_1 of the oscillators 3, 5, 7, 10, 13, 15, 17, 19, and 20 compared to state x_1 of oscillator 1. The phase plane depicts synchronization among the oscillators. Note that only a fraction of the oscillators were compared. These were picked arbitrary and for space purposes. Also note that the synchronization transitory was omitted.

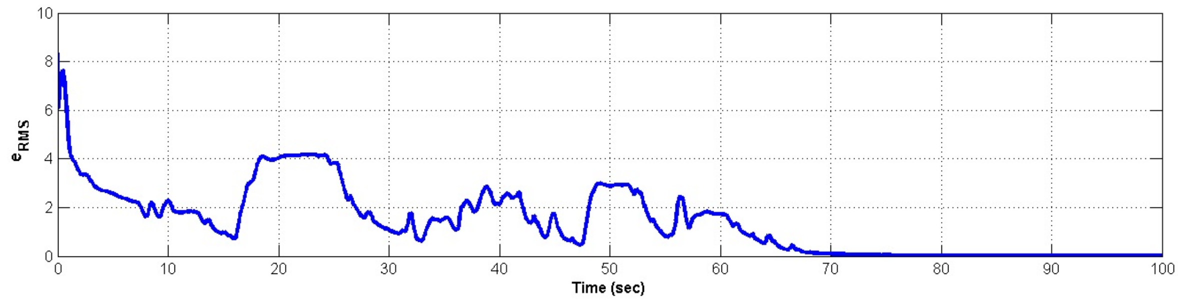

FIGURE 4. Root mean squared error e_{RMS} of the dynamics of every oscillator on the network. Note that only the first 100 seconds are shown.

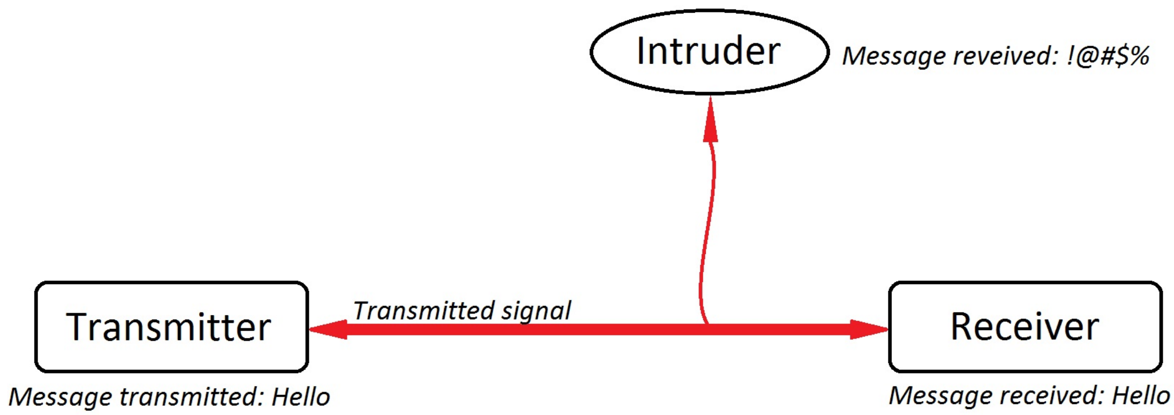

FIGURE 5. Example of encryption, were an intruder cannot make sense of the message.

The initial conditions were selected arbitrary, and can be seen in Table I. In order for the dynamics of the oscillators to achieve synchronization as in Eq. (2), the vector K was determined as in Theorem 3.2. As a result the parameter gains are: $K_1 = 5.27$, $K_2 = -1.1002$, $K_3 = 0.00122$. The following gradient vectors were used as well:

$$\frac{\partial H}{\partial x_1} = \begin{bmatrix} x_{i,1} \\ x_{i,2} \\ \varepsilon x_{i,3} \end{bmatrix}, \qquad i = 1, 2, ..., 20. \qquad (18)$$

A diagonal line in the phase graph, as shown in the Fig. 3, means that synchronization is achieved after a finite period of time. This shows that synchronization in every $x_{i,1}$, $i = 1, 2, ..., 20$ is obtained, hence Eq. (2) holds. The Fig. 4 shows the root mean squared error e_{RMS}, expressed in Eq. (5), of all the states $(x_{i,1}, x_{i,2}, x_{i,3})$ of every oscillator i in the network. It can be seen that all states synchronize and the network experience complete synchronization after a finite period of time. The states $x_1(t)$, $x_2(t)$, and $x_3(t)$ of all oscillators can be shown in Fig. 8 in sections e), f), and g) respectively, in which only the first 120 seconds are shown for representative purposes.

TABLE I. Initial conditions of each oscillator.

$x_1(0)=(5, -7.2, 1.5)$	$x_{11}(0)=(0, -0.09, 0)$
$x_2(0)=(8, 2.5, -1.2)$	$x_{12}(0)=(-1.9, 3.22, 3.75)$
$x_3(0)=(0.53, 0.1, 0.26)$	$x_{13}(0)=(0.5, 1.12, 6.62)$
$x_4(0)=(1, 0, 1)$	$x_{14}(0)=(1, 0, -1)$
$x_5(0)=(6.5, 4.9, 3.1)$	$x_{15}(0)=(-1, 1, 0.4)$
$x_6(0)=(-9, -1.2, -3.7)$	$x_{16}(0)=(0.9, -3.712, 4.07)$
$x_7(0)=(17, -2.1, 1)$	$x_{17}(0)=(-0.9, 0.8, 1.31)$
$x_8(0)=(5.5, -1.451, 3.6)$	$x_{18}(0)=(0.8, 1.1, 6.61)$
$x_9(0)=(1, -9.01, 0.1)$	$x_{19}(0)=(1, -0.1, 0.1)$
$x_{10}(0)=(-6.57, 2.479, -0.31)$	$x_{20}(0)=(0.8, -0.8, 3.9)$

6. Chaotic encryption

Whether is used by the military or securing bank accounts, many forms of encryption have been developed throughout history. Decryption developed as a way of finding out what the encrypted data meant, see Fig. 5. As a result, the newest

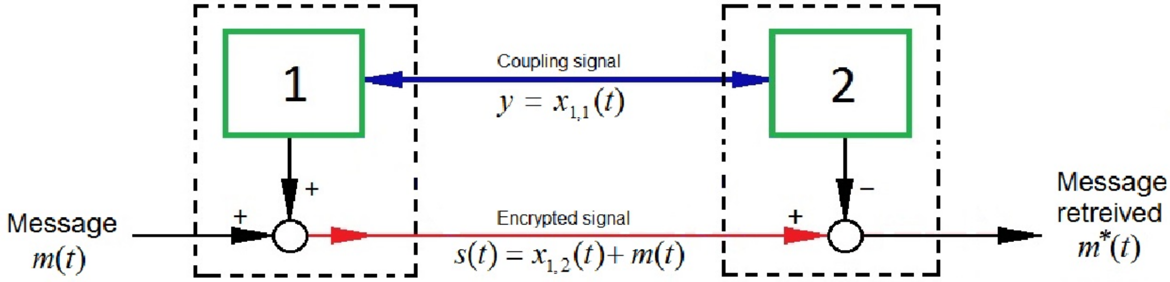

FIGURE 6. General diagram for the chaotic communication scheme with two transmission channels. Note that for the simulation 20 oscillators is used. $m(t)$ is the message to be transmitted, which will be added a chaotic dynamic $x_{1,2}(t)$. Now the encrypted signal $s(t)$ is obtained. A chaotic dynamic from a different oscillator $x_{2,2}(t)$ will be subtracted to $s(t)$, as a means to retrieve a message $m^*(t)$. To ensure that the dynamic $x_{1,2}(t)$ and $x_{2,2}(t)$ are the same, a coupling signal is send from one oscillator to the other to synchronize them.

cryptosystem must be better that the previous one by “outsmarting” decryption; and vice-versa. Chaotic synchronization can be used as a technique for encrypting data. Masking signal with chaotic synchronization was suggested by Cuomo in 1992 [4].

6.1. Additive encryption with two channels

For this type of encryption, the original message $m(t)$ is added to the coupling signal produced by a chaotic oscillator, in this case $y = x_{1,2}(t)$. The encrypted signal will be:

$$s(t) = x_{1,1}(t) + m(t). \tag{19}$$

This encrypted signal can be decrypted by other chaotic oscillator, but only if both oscillators have exactly the same dynamic regardless of their original initial conditions. To ensure this, a coupling signal $x_{1,1}$ is send among oscillators so they can synchronize as in Eq. (10), see Fig. 6. According to (2), the original chaotic signal $x_{1,2}(t)$ and the synchronized signal $x_{2,2}(t)$ should have the same dynamic $x_{1,2}(t) = x_{2,2}(t)$. This means that the message can be obtained by subtracting the chaotic signal $x_{2,2}(t)$ from the encrypted message $s(t)$, as follows:

$$m^*(t) = s(t) - x_{2,2}(t). \tag{20}$$

So then:

$$m^*(t) = m(t). \tag{21}$$

This same principle was used using 20 oscillators all coupled as in Fig. 2. For encryption, we could have used any kind of data; in this case we are using an image, a painting from famous author Remedios Varo, see Fig. 7. It is a 264×216 pixels picture, of approximately 110 KB, in PNG format.

Before an encryption is done, a brief introduction to the kind of data to be encrypted is explained. Digital images are made of pixels, which are the smallest controllable element of a picture. Each pixel contains a code referring to color. For a colored image, a 3 dimensional information matrix $M \times N \times P$ can be obtained. In these case P gives back

FIGURE 7. “Creación de las aves” (Bird creation), 1957. Author: Remedios Varo. Original PNG image to be encrypted.

information about the color. P can be either 3 or 4 character if the image is using a 8-bit or 16-bit color format, according to Matlab specifics. Basically, for this encryption scheme, the matrix $M \times N \times P$ is turned into a signal, see Fig. 8d. This signal will be used as our original message $m(t)$. Although, signal masking or additive encryption will not work if the masking signal $y = x_{1,2}(t)$ is proportionally low to the original message $m(t)$. For this case, the masking signal was multiplied 10 times. If this is not done, the resulting encrypted message will still be visible, but with perturbations (resulting from the chaotic masking signal).

7. Results on the chaotic encryption

In Fig. 8 the results of the synchronization and the encryptions scheme can be seen. As explained before, the image (see Fig. 8a) is changed to a signal or message $m(t)$ as can be seen in Fig. 8d. Before encrypting the image, the 20 oscillators are coupled and synchronized as proved with the phase plane in Fig. 3. Synchronization among the states $x_{i,1}(t)$, $x_{i,2}(t)$, and $x_{i,3}(t)$, is achieved in the first 120 seconds, see Fig. 8e, 8f, and 8g. Past this transition

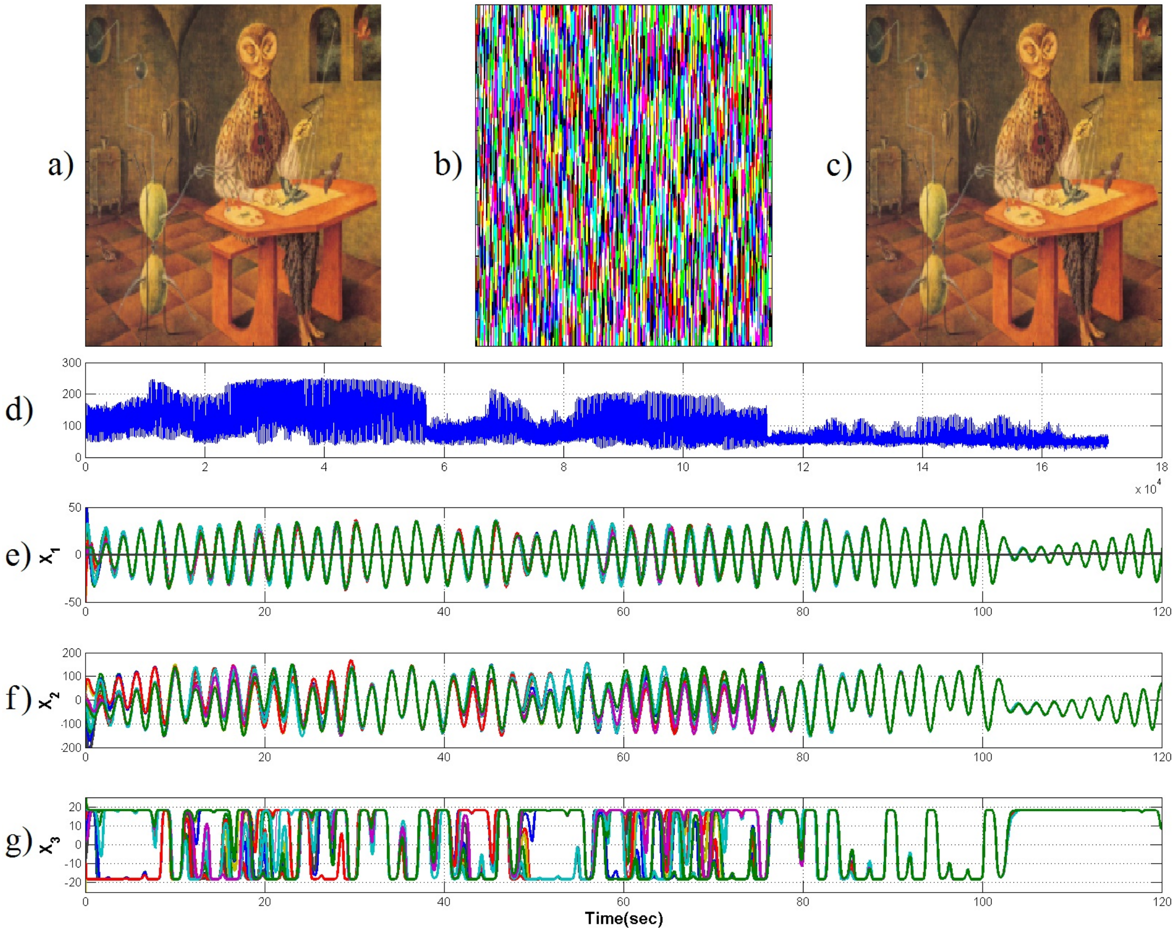

FIGURE 8. a) Depicts the original painting to be encrypted; b) reconstructed image after encryption $s(t) = x_{1,2}(t) + m(t)$; c) image reconstructed from oscillator 2 by $m^*(t) = s(t) - x_{2,2}(t)$. Note that the reconstructed image from oscillator 3 to 20 are the same as in oscillator 2, so then they are not shown. d) Signal produced by reshaping the image, $m(t)$; e), f), and g) show the evolution and synchronization of the states $x_{i,1}(t)$, $x_{i,2}(t)$, and $x_{i,3}(t)$ respectively, of the oscillators 1 through 20. Note that only the first 120 seconds are shown for representative purposes and that in e) the black line represents the message to be encrypted $m(t)$ as it starts after the synchronization is completed.

time, the image is encrypted adding the chaotic signal as in $s(t) = x_{1,2}(t) + m(t)$, and the encrypted image retrieved is in Fig. 8b. Finally, the signal is decrypted subtracting a chaotic signal produced by any oscillator, in this case oscillator 2, as in $m^*(t) = s(t) - x_{2,2}(t)$. The image retrieved by the message $m^*(t)$ can be seen in Fig. 8c; revealing a perfect match with the original.

8. Conclusion

For some time the generalized Hamiltonian approach was used exclusively to synchronize two chaotic oscillators in a unidirectional master-slave array. In this paper synchronization was achieved in an irregular arrayed network in their generalized Hamiltonian form. Then it was shown its potential in data encryption using an image. This can give new insights, about the construction of the oscillators and networks. Many other chaotic oscillators in generalized Hamiltonian form can be used. Recent studies on synchronization of complex dynamical networks may shed new light on behavior and understanding of synchronization itself or complexity in network dynamics.

Acknowledgments

This work was supported by CONACYT, México under Research Grant No. 166654.

1. C. Cruz-Hernández, *Nonlinear Dyn. Syst. Theory* **4** (2004) 1.
2. X. Wu, G. Chen, and J. Cai, *Phys. D* **229** (2007) 52.
3. L. M. Pecora and T. L. Carroll, *Phys. Rev. Lett.* **64** (1990) 821.
4. K. M. Cuomo, A. V. Oppenheim, and S. H. Strogatz, *IEEE Trans. Circuits Syst. II, Analog Digit. Signal Process*. **40** (1993) 626.
5. P. Grigolini, P. Hamilton, J. Roberts, and B. J. West, *Chaos, Solitons & Fractals* **20** (2004) 1.
6. P. Grigolini, P. Allegrini, and B. J. West, *Chaos, Solitons & Fractals* **34** (2007) 3.
7. M.E. Newman, *Phys. Rev. E* **64** (2001) 016131.
8. S. Redner, *EPJ B* **4** (1998) 131.
9. J. Scott, *Sociology* **22** (1988) 109.
10. J. Galaskiewicz and S. Wasserman, *Sociological Methods & Research* **22** (1993) 3.
11. J. Cohen, T. Jonsson, and S. R. Carpenter, *Proc. Nat. Acad. Sc.* **100** (2003) 1781.
12. E. Ravasz, A. L. Somera, D. A. Mongru, Z. N. Oltvai, and A.-L. Barabási, *Science* **297** (2002) 1551.
13. J. White, E. Southgate, J. Thomson, and S. Brenner, *Phil. Trans. R. Soc. Lond* **314** (1986) 1.
14. L. Kocarev, K. Halle, K. Eckert, L.O. Chua, and U. Parlitz, *Int. J. Bifurc. Chaos* **2** (1992) 709.
15. L. Cardoza-Avendano *et al*., *Rev. Mex. Fis* **58** (2012) 472.
16. J.L. Mata-Machuca, R. Martínez-Guerra, R. Aguilar-López, and C. Aguilar-Iba nez, *Commun. Nonlinear Sci. Numer. Simulat.* **17** (2012) 1706.
17. R. Núñez-Pérez, *Rev. Mex. Fis.* **52** (2006) 464.
18. C. Tao and G. Du, *Int. J. Bifurc. Chaos 13* (2003) 2689.
19. G. Pérez and H. A. Cerdeira, *Phys. Rev. Lett.* **74** (1995) 1970.
20. A. Aguilar-Bustos and C. Cruz-Hernández, *Chaos, Solitons & Fractals* **41** (2009) 1301.
21. J.-P. Goedgebuer, L. Larger, and H. Porte, *Phys. Rev. Lett.* **80** (1998) 2249.
22. N. Smaoui, A. Karouma, and M. Zribi, *Commun. Nonlinear Sci. Numer. Simulat.* **16** (2011) 3279.
23. J. Lü and G. Chen, *Int. J. Bifurc. Chaos* **16** (2006) 775.
24. L. Gámez-Guzmán, C. Cruz-Hernández, R. López-Gutiérrez, and E. García-Guerrero, *Rev. Mex. Fis* **299** (2008) 54.
25. Y. Tang and J. Fang, *Commun. Nonlinear Sci. Numer. Simulat.* **15** (2010) 401.
26. X. Wu, H. Wang, and H. Lu, *Nonlinear. Anal. Real App.* **13** (2012) 1441.
27. A. Kiani-B, K. Fallahi, N. Pariz, and H. Leung, *Commun. Nonlinear Sci. Numer. Simulat.* **14** (2009) 863.
28. C. Cruz-Hernández, in *Procs. of the IASTED on Circuits, Signal, and Systems* (2002).
29. D. López-Mancilla, C. Cruz-Hernández, and C. Posadas-Castillo, in *Journal of Physics: Conference Series*, **23** (IOPublishing, 2005) p. 267.
30. C. Posadas-Castillo, E. Garza-González, D. Diaz-Romero, E. Alcorta-García, and C. Cruz-Hernández, *J. Appl. Res. Technol*. **12** (2014) 782.
31. H. Sira-Ramirez and C. Cruz-Hernández, *Int. J. Bifurc. Chaos* **11** (2001) 1381.
32. X. F. Wang, *Int. J. Bifurc. Chaos* **12** (2002) 885.
33. S. Boccaletti, J. Kurths, G. Osipov, D. Valladares, and C. Zhou, *Phys. Rep.* **366** (2002) 1.
34. J. Wang and Y. Zhang, *Phys. Let. A* **374** (2010) 1464.